MJFAS MALAYSIAN JOURNAL OF FUNDAMENTAL AND APPLIED SCIENCES
PRINT ISSN: 2289-5981 | ONLINE ISSN: 2289-599X

RESEARCH ARTICLE

Decolorization of Reactive Black 5 dye using gel combustion synthesized $LaFeO_3$ nanoparticles

Arif Aizat [a], Farhana Aziz [a, *], Mohd Zamri Mohd Yusop [a, b], Juhana Jaafar [a], Norhaniza Yusof [a], Wan Norhayati Wan Salleh [a], Ahmad Fauzi Ismail [a]

[a] *Advanced Membrane Technology Research Centre (AMTEC), School of Chemical and Energy Engineering, Faculty of Engineering, Universiti Teknologi Malaysia, 81310, UTM Skudai, Johor, Malaysia*

[b] *Department of Materials, Manufacturing and Industrial Engineering, School of Mechanical Engineering, Faculty of Engineering, Universiti Teknologi Malaysia, 81310 UTM Skudai, Johor, Malaysia*

* *Corresponding author: farhanaaziz@petroleum.utm.my*

Article history
Received 5 January 2019
Revised 14 February 2019
Accepted 11 March 2019
Published Online 25 June 2019

Abstract

Lanthanum orthoferrite ($LaFeO_3$) nanoparticles was prepared via gel combustion method with fixed reaction temperature at 200°C, but different reaction time of (t) 2 hours (t=2h) and 24 hours (t=24h), respectively. Physicochemical properties' characterization was performed to compare both samples. UV-Vis spectroscopy analysis was done to determine the photocatalytic performance on Reactive Black 5 (RB5) dye. $LaFeO_3$(t=24h) possessed a high crystallinity structure with specific surface area (SSA) of 28.037 m^2g^{-1}, while $LaFeO_3$(t=2h) had a mixture of crystalline and amorphous structures with SSA of 40.952 m^2g^{-1}. The catalysts' loading was also varied in a few conditions to elucidate the optimum loading that maximize the dye removal by mean of adsorption-photocatalytic action. Up to 94% of RB5 dye was successfully removed within 6h by $LaFeO_3$(t=2h) samples, and this enhanced synergistic activity of $LaFeO_3$ is promising for the further application of visible light driven photocatalyst in polluted water treatment.

Keywords: Lanthanum orthoferrite, combustion method, reaction time, photocatalysis, dye degradation

INTRODUCTION

Photocatalysis embark the principle of free radicals production by creating electron-hole pairs as the light absorbed. The release of hydroxyl radicals, •OH degrade and/or degenerate contaminants completely and effectively [1]. Even if there are side products formed, typically they are non-hazardous and chemically less active compared to the initial contaminants constituents [2]. Perovskites, a collective name for materials with orthorhombic crystalline structure of ABO_3 (A=typically rare-earth elements; B=transition metals) is a promising candidate of photocatalysts. Lanthanum orthoferrite, $LaFeO_3$ is an example of compound with perovskite structure that had been studied for it photocatalytic activity in wastewater treatment. $LaFeO_3$ possess a narrow band gap of 1.86 to 2.36 eV, making it efficient in visible light region. Furthermore, it stability and non-toxicity properties made it a promising material in wastewater treatment [3].

The synthesis of $LaFeO_3$ can be carried out via multiple methods, such as hydrothermal synthesis, sol-gel method, co-precipitation method and solution combustion method. With the same goal of synthesizing an orthorhombic crystalline structure of $LaFeO_3$ nanoparticles with high surface area and exceptionally good photocatalytic activity, they can be differentiated by the amount of energy used in synthesis process [4]. High calcination temperature, long complexing duration, high amount of reactants used and the formation of unwanted by-products are some of the problems encountered that justify the extra amount of energy needed and these may not be efficient, especially in industrial scale [5,6].

Gel combustion synthesis is one of the interesting methods that can be used to synthesize metal oxides, and it is easily scalable to fit industrial need. Based on the rapid exothermic reactions between the premixed metal nitrates with sacrificial or complexing agent, the gelation process followed by low reaction temperature will induce the oxidation-reduction reaction to produce well-crystalline structured nanomaterials with large surface area [7]. Moreover, this method is simple, cost-effective and easy compared to other methods. Numerous researchers had reported the successful synthesis of $LaFeO_3$ by gel combustion synthesis and the effect of reaction temperature towards the physicochemical properties of the nanomaterials [7–9]. However, limited studies have been made regarding the effect of reaction period at specified temperature.

We hereby reported the successful synthesis of $LaFeO_3$ nanoparticles by gel combustion method with citric acid as sacrificial agent at reaction temperature of 200°C. By varying the reaction time at 2h and 24h, the physicochemical properties of the synthesized nanoparticles were thoroughly compared. Furthermore, experimental procedure using Reactive Black 5, RB5 dyes for dye degradation was carried out to determine the efficiency of synergistic adsorption-degradation activity of $LaFeO_3$ nanoparticles synthesized.

EXPERIMENTAL

Materials

Methods for $LaFeO_3$ nanoparticles synthesis

Analytical grade Lanthanum (III) nitrate hexahydrate, $La(NO_3)_3{\cdot}6H_2O$, iron (III) nitrate nonahydrate, $Fe(NO_3)_3.9H_2O$ and citric acid monohydrate ($C_6H_8O_7.H_2O$) were purchased from Sigma-Aldrich Ltd. According to stoichiometric preparation of lanthanum

orthoferrite, $LaFeO_3$, the calculated amount of $La(NO_3)_3{\cdot}6H_2O$ and $Fe(NO_3)_3{\cdot}9H_2O$ were dissolved in citric acid solution at 60°C under constant stirring. The amount of citric acid needed was equal to the molar amount of metal nitrates in the solution. As both metal nitrates visually dissolved, 25% ammonia solution was added dropwise to adjust the pH to 7 and subsequently stabilize the sol. The nitrate-citrate sol was then poured into ceramic crucible and heated slowly to 120°C. The changes in viscosity and color of the sol to brown confirmed the formation of dry gel. The dry gel was later subjected to react at 200°C for 2 hours (*t*=2h) and 24 hours (*t*=24h). This activation process transformed the dry gel into loose powder. The obtained as-synthesis powder was the $LaFeO_3$ nanocrystalline with fine crystal powder and no further calcination at high temperature needed.

Methods of characterization

The crystalline structure of the synthesized $LaFeO_3$ samples were characterized by X-ray powder diffraction (XRD, PANalytical XPERT-PRO) using Cu Kα radiation (*λ*=1.5406 Å) at 45 kV. Brunauer–Emmett–Teller (BET) surface area analysis was carried out using BELSORP-max Ver 1.3.0 instrument by mean of N_2 adsorption at -196.15°C. Morphologies, corresponding with selected area electron diffraction (SAED) and Energy Dispersive X-Ray spectroscopy (EDS) of the samples were observed using transmission electron microscopy (TEM, JEOL JEM-ARM200F ACCELARM Atomic Resolution Analytical Electron Microscope).

RB5 dyes adsorption and degradation

The adsorption and photocatalytic degradation activities of as-synthesis $LaFeO_3$ nanoparticles' samples were studied using Reactive Black 5 ($C_{26}H_{21}N_5Na_4O_{19}S_6$) azo dye in customized photo reactor. About 1 g/L of $LaFeO_3$ nanoparticles were suspended in RB5 dye solution with 10 ml/L of 3% hydrogen peroxide that act as degradation catalyst. The initial concentration of RB5 dye solution was kept at 30 mg/L. The beaker was continuously stirred to prohibit the settling of nanoparticles at the bottom of the beaker. For the first couple hours, the beaker was kept in the dark for $LaFeO_3$ nanoparticles to establish the absorption-desorption equilibrium. Following that, the mixture was irradiated with 100W LED light as the source of visible light for 4 hours. Aliquots were obtained for analysis every 60 minutes using 0.45µm filtered syringe to hinder the presence of nanoparticles in samples. The analysis was carried out to monitor the concentration of RB5 dye by determining the absorbance value using UV-Vis spectrophotometer. Throughout the experiment, the temperature and pH of the dye solution were monitored. The experiment was repeated with 2g/L and 3g/L $LaFeO_3$ suspension. The adsorption and photocatalytic performance of $LaFeO_3$ nanoparticles were later evaluated by using the formula:

$$\textit{Removal of RB5 dye (in \%)} = ((C_0 - C_t / C_0) * 100 \quad (1)$$

where C_0 and C_t is the initial and final concentration of dye (in mg/L), respectively.

RESULTS AND DISCUSSION

Characterization

To determine the crystalline structure of the synthesized $LaFeO_3$ samples with different reaction times of activation, the XRD patterns are shown in Figure 1. The samples reacted for 24h ($LaFeO_3$ (*t*=24h)) (Figure 1(a)) displayed a pure perovskite structure with orthorhombic phase peaks, that can be indexed based to powder diffraction file (JCPDS card no. 37-1493). No possible impurities nor contamination can be observed, suggesting that the single-phase $LaFeO_3$ is successfully synthesized when the reaction time was set at 24 hours. However, the $LaFeO_3$ samples synthesized under 2h of reaction time at 200°C ($LaFeO_3$ (*t*=2h)) showed lower peaks' intensity, suggesting that the samples is not a single-phase $LaFeO_3$, but the mixture of crystalline and amorphous state materials. The enhanced look of 121 diffraction peaks (Figure 1(c)) showed that the differences in reaction time will affect the crystallinity of the samples, as $LaFeO_3$ (*t*=24h) samples show narrower and intense peak compared to broader and less intense $LaFeO_3$ (*t*=2h) samples. This is deduced based on the study carried out by Yin *et al.*[10]. They demonstrated that increase in reaction time will enhance selective crystal growth of amorphous-state TiO_2 to crystalline-state, introducing stronger crystalline peaks in the XRD patterns. Moreover, the presence of sacrificial/complexing agent such as citric acid will further promote the crystallization process, postulate to be caused by face-sharing polycondensation mechanism of the protonated metals used due to acid catalysis. On the other hand, the pseudo-particle size of both samples was then calculated based on the Scherrer formula:

$$\tau = K\lambda/\beta \cos\theta \quad (2)$$

where τ is mean pseudo-size of particles, K is 0.9, λ (Kα wavelength) is 0.1541 nm, β is full width at half maximum of (121) diffraction peak, in radian, and θ is the Bragg angle of the peak (in degree). It was estimated that particle size of $LaFeO_3$ (*t*=24h) and $LaFeO_3$ (*t*=2h) to be 32.229 nm and 20.066 nm, respectively.

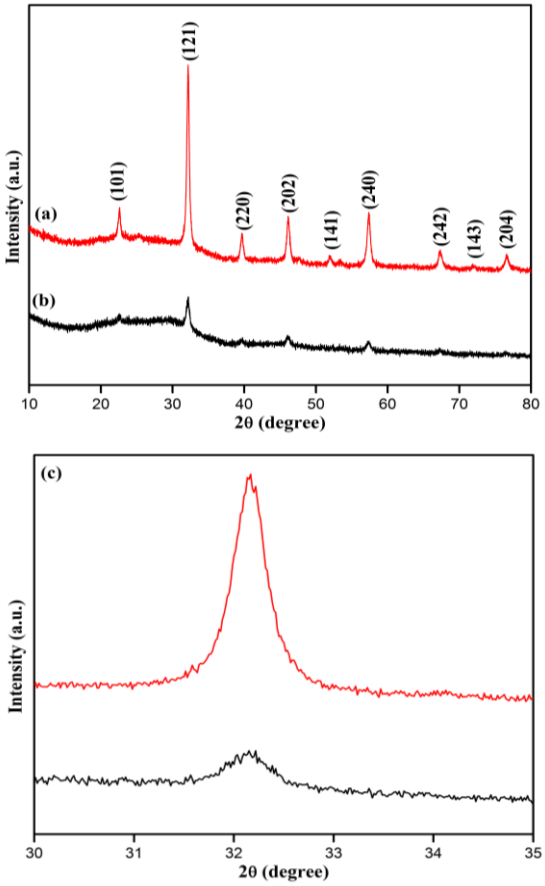

Fig. 1 XRD spectra of: (a) $LaFeO_3$ (*t*=24h), (b) $LaFeO_3$ (*t*=2h) and (c) detailed 121 peaks of both samples.

The BET surface analysis is carried out to confirm that the synthesized $LaFeO_3$ nanoparticles showed the inversed co-relation between the mean particle size and specific surface area (SSA), as represented in Table 1. The small mean particle size of $LaFeO_3$ (*t*=2h) has an exceptionally higher SSA of 40.952 m^2g^{-1}, compared to $LaFeO_3$ (*t*=24h) (28.037 m^2g^{-1}). This showed that the reaction time affected the structural constituents of $LaFeO_3$ samples produced. Furthermore, the reaction time will also affect the total pore volume of formed particles. Based on a study carried out by Shikha and colleagues, synthesis of nanoparticles by combustion method leads to the formation of porous structure with increased surface area [11].

Table 1 BET analysis of both samples with different reaction time.

Sample	Specific Surface Area (m^2g^{-1})
$LaFeO_3$ (*t*=2h)	40.952
$LaFeO_3$ (*t*=24h)	28.037

To study the structural difference between the two samples of $LaFeO_3$ nanoparticles synthesized, high resolution TEM (HRTEM) was carried out and the images are shown in Figure 2. $LaFeO_3$ (*t*=2h) samples exhibited mixture of amorphous and crystalline structure, with calculated lattice spacing of 0.205 nm (Figure 2 a, c). Figure 2c shows mixture of small particles (size approximately 20 – 50 nm) and amorphous structure. On the other hand, synthesized $LaFeO_3$ that had been activated for 24h at 200°C show random particles size with crystalline structure (Figure 2b). HRTEM image (Figure 2d) shows a uniform lattice fringe with an interplanar *d*-spacing of 0.272 nm assigned to (121) lattice planar, suggesting the formation of high quality orthorhombically-structured $LaFeO_3$ nanoparticles. On the other hand, the selected area electron diffraction (SAED) images obtained from the interplanar *d*-spacing area confirmed the orthorhombic structure of both $LaFeO_3$ samples can be indexed to standard powder diffraction data (JCPDS card no. 37-1493). Concurrently, the elemental characterization of the both samples is also carried out by EDS analysis and showed that the elemental composition of $LaFeO_3$ nanoparticles synthesized by both reaction times consisted of La, Fe and O in stoichiometric molar ratio of 1:1:3. These findings are important to highlight the purity of both samples and the unchanged composition of $LaFeO_3$ even though the reaction time may interfer the crystallinity of the samples.

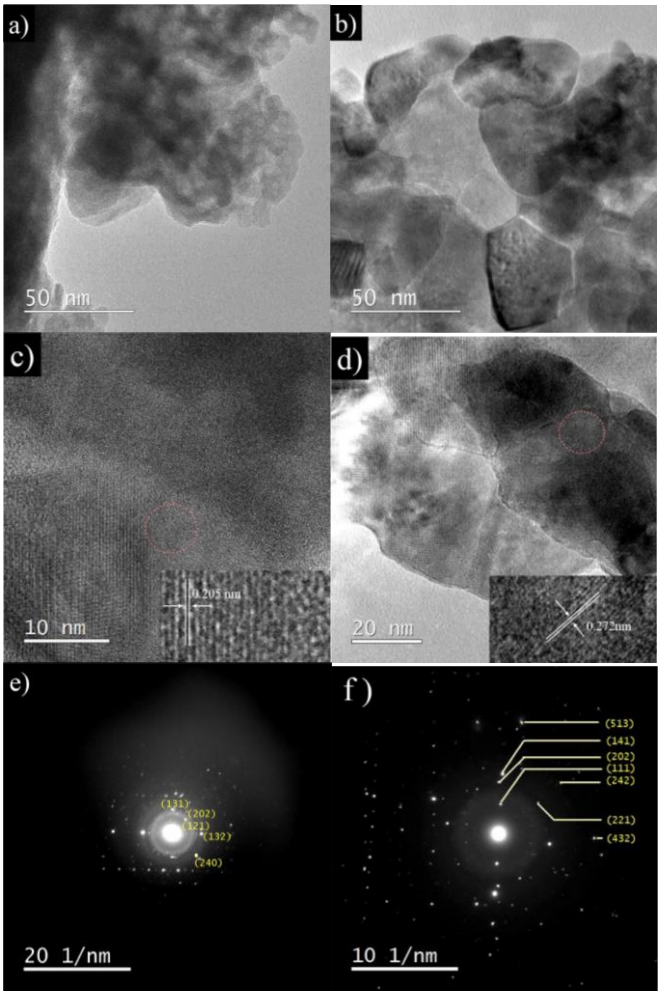

Fig. 2 TEM images of (a, c) $LaFeO_3$ (*t*=2h) and (b, d) $LaFeO_3$ (*t*=24h) and electron diffraction of (e) $LaFeO_3$ (*t*=2h) and (f) $LaFeO_3$ (*t*=24h).

Photocatalytic activities

The performance of both $LaFeO_3$ samples is evaluated by photocatalytic degradation of Reactive Black 5 (RB5) dye. Based on Figure 3, the photolysis of RB5 with 3% hydrogen peroxide leads to a very low reduction (8.33%). On the other hand, with the presence of $LaFeO_3$ nanoparticles, higher activity of RB5 removal by mean of photocatalytic degradation can be clearly observed. Two hours prior to irradiation of visible light, the concentration of the dye shows relatively high reduction, mainly due to the adsorption of dye compound onto the surface of $LaFeO_3$ nanoparticles. However, both samples exhibited different adsorption capability, as $LaFeO_3$ (*t*=2h) showed higher adsorption of RB5 dye for the first two hours with 54.97% of dye compounds were adsorbed onto its surface. This occured mainly due to the crystalline-amorphous state of the samples, leading to higher SSA compared to $LaFeO_3$ (*t*=24h) samples which eventually provide more active sites on the surface of the nanoparticles [2]. Conversely, $LaFeO_3$ (*t*=24h) nanocrystalline showed lower adsorption capacity with only 33.09% dye compounds were removed under dark condition through adsorption process.

High adsorption capacity of organic contaminants onto the surface of photocatalysts is important to be considered, based on the study carried out by Zhu *et al.* [12]. They fabricated polythiophene/titanium oxide composites with high adsorption capacity, adsorbing 63.8% of methyl orange dye within 60 minutes in the absence of any light. Beside the SSA factor, high adsorption capacity of photocatalysts was also contributed by the charges difference between photocatalysts' surface and the contaminants. Positively-charged $LaFeO_3$ nanoparticles' surface can strongly adsorb negatively-charged RB5 dye by electrostatic interactions, eventually facilitate an efficient interfacial charge transfer when photocatalytic degradation takes place [13]. As irradiation of visible light took place, the photodegradation of RB5 dye was initiated, and subsequently increase the removal rate by catalyzing adsorbed dye compounds on the surface of $LaFeO_3$ nanoparticles.

This action can be explained in terms of a high photo transformation quantum yield, where the reactive excited states activate through photochemical processes [1]. Both samples show potential to harvest light in the visible light region, so that the yield of radicals available for dye removal is higher. However, it can be clearly observed that $LaFeO_3$ (*t*=24h) samples showed higher photocatalytic activity. Within the 1st hour of irradiation, 15.2% of RB5 compounds is further removed by mean of photocatalysis and the degradation continues to occur within the allocated time to a total of 61.84% removal. Contrarywise, $LaFeO_3$ (*t*=2h) samples only showed slight photocatalytic activity after irradiation, accounted at 7.2% for final removal percentage of 62.17%. Higher SSA of $LaFeO_3$ (*t*=2h) samples ~~is~~ hypothesized to cause this as higher amount of dye molecules or carbon contaminants adsorbed onto the surface of photocatalysts will subsequently block the active sites, causing reduction in the nanoparticles' activity to produce radicals as lower number of photons can be absorbed to initiate the catalytic process [14].

These results also showed that the synergistic act of adsorption and degradation is favorable in the use heterogenous photocatalyst as this will increase the effectiveness of the process, compared to the usage of radical-forming agents such as hydrogen peroxide only. Adsorption of the dye molecules onto the available active sites on the surface of $LaFeO_3$ catalysts will maximize the contact time for OH• and $O_2^{\bullet-}$ radicals generated to completely mineralize the dyes without formation of intermediate compounds, as long as the photocatalyst' surface are not entirely blocked. The degradation path of RB5 by $LaFeO_3$ nanoparticles is postulated to follow Equation (3) to (7), based on the pathways suggested by Shanavas *et al.* [15]:

$$LaFeO_3 + h\nu \rightarrow LaFeO_3\ (e_{CB}^- + h_{VB}^+) \quad (3)$$

$$LaFeO_3\ (h_{VB}^+) + OH \rightarrow OH\bullet \quad (4)$$

$$LaFeO_3\ (e_{CB}^-) + O_2 \rightarrow O_2^-\bullet \quad (5)$$

$$O_2^-\bullet + H_2O \rightarrow HO_2^-\bullet + OH^- \quad (6)$$

$$(OH\bullet + O_2^-\bullet + HO_2^-\bullet) + RB5 \rightarrow CO_2 + H_2O \quad (7)$$

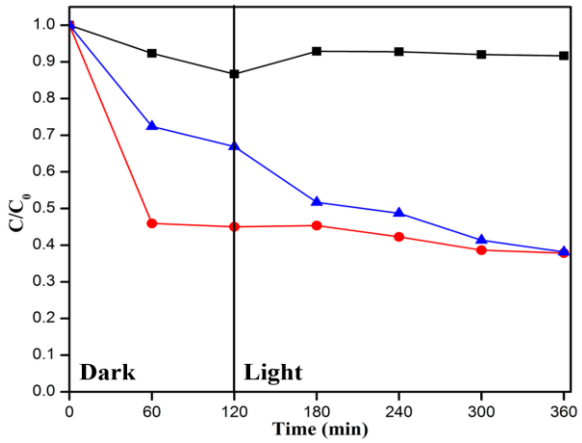

Fig. 3 RB5 dye removal by 3% hydrogen peroxide (control) (■), $LaFeO_3$ (*t*=2h) (•) and $LaFeO_3$ (*t*=24h) (▲).

Effect of catalysts loading

Optimum catalyst loading determination is crucial in heterogenous photocatalytic reaction due to two main reasons; (1) to prevent excessive usage of catalysts leading to higher processing cost, and (2) to optimize the amount of photons adsorbed onto the surface of the catalysts so photocatalytic process can take place [16]. The later one is important as excessive catalyst loading will subsequently increase turbidity of the suspension, reducing light penetration and promoting light scattering, resulting in the reduction of activated sites on the photocatalyst surface, thus reducing the overall performance of the process [17].

Potrayed in Figure 4, the loading of both $LaFeO_3$ samples were varied to 1g/L, 2g/L and 3g/L. As discussed before, 1g/L loading of both $LaFeO_3$ (*t*=2h) and $LaFeO_3$ (*t*=24h) nanoparticles resulted an exceptional removal of RB5 dye at 62.17% and 61.84%, respectively. However, the rate of RB5 removal was found to be increased as the amount of catalysts used increased to 2g/L. Increased by 11.09% to 73.26% for $LaFeO_3$ (*t*=2h) nanoparticles, 2g/L of the crystalline-amorphous samples showed different trend of dye removal, where desorption occurred within the first hour of irradiation, followed by steady reduction of dye molecules afterwards. On contrary, 3g/L loading of $LaFeO_3$ (*t*=2h) nanoparticles showed a significant reduction of RB5 concentration two hours after irradiation occurred, successfully removing 94.39% of dye compounds by synergistic act of adsorption-photocatalysis (Figure 4a). For $LaFeO_3$ (*t*=24h) nanocrystalline samples, results also depicted that increasing the catalyst loading consequently increase the rate of RB5 dye removal (72.01% and 96.2% for 2g/L and 3g/L loading, respectively) (Figure 4b).

It is also worth noted that the adsorption of RB5 dye molecules onto the surface of photocatalyst within the first two hours prior to irradiation increased as the catalyst loading increased, and the occurrence took place in both samples. This can be graphically explained by the increasing interaction between photocatalyst and the organic contaminants, as illustrated in Figure 5. Increasing the amount of catalysts into the fixed concentration of contaminants in wastewater will provide more active sites, which can be found on the surface of photocatalyst. Increasing number of active sites ensure higher chance for the contaminants to be adsorbed onto the photocatalyst's surface, thus resulting a sharp decrease in concentration of dye (organic contaminants) within the first hour of interaction, with the absence of photocatalysis process. However, based on a study carried out by Shet and Shetty K [17], if the loading of photocatalyst is too high, photodegradation/photocatalysis process will decrease as there is high possibility of nanoparticles' agglomeration, reducing the surface area for photo-absorption, and subsequently reducing the number of vacant active sites.

Nevertheless, neither $LaFeO_3$ samples demonstrate high degree of particles' agglomeration when the amount of nanoparticles introduced in the aquoeus environment increased, and this is deduced based on the fact that higher loading of catalysts lead to higher removal of dye compound. This is contributed by several factors, including the combustion method used to synthesize $LaFeO_3$ samples. According to Shikha *et al.* [11], due to rapid combustion of metal precursors in the presence of organic fuel such as citric acid, the nucleation rate of nanoparticles prepared are better compared to other conventional techniques, leading to more pronounced and uniformed crystalline structure with little aggretation and agglomeration between nanoparticles. Uniformity of nanoparticles' structure cause them to disperse evenly in aqueous medium, thus the formation of agglomerated samples will not exist. Another theory that can be considered is the presence of Coulomb repulsion forces that hindered the agglomeration due to the equal energy state of nanoparticles. Moreover, as the agglomeration of nanoparticles may happen in real life situation, the agglomeration can only occur via surface-cluster-surface mechanism, and not surface-surface mechanism as commonly believed; where the existence of supercritical clusters took place because of incomplete reaction or growth of reactants by condensation [18].

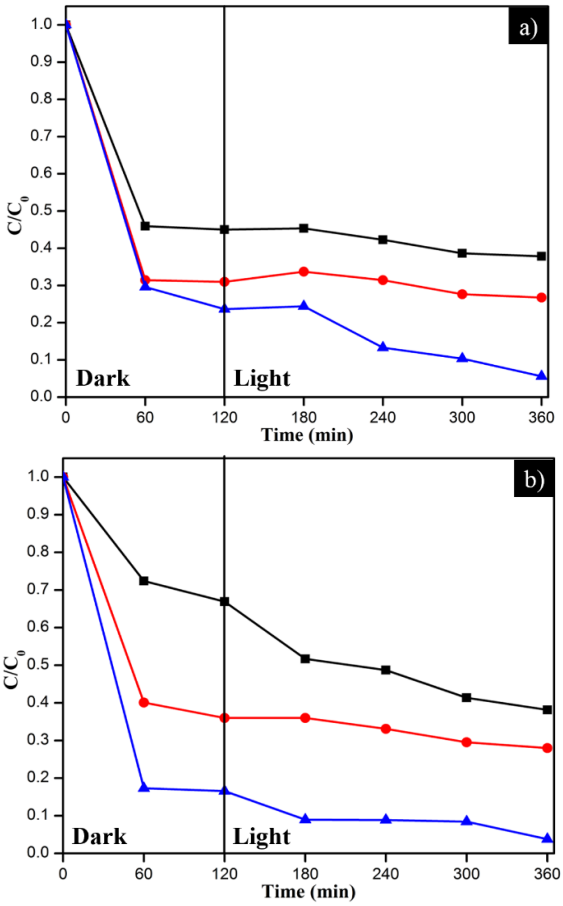

Fig. 4 Effect of $LaFeO_3$ loading on removal efficiency of RB5 dye, where (a) is $LaFeO_3$ (*t*=2h) samples, (b) is $LaFeO_3$ (*t*=24h) samples, (■) is 1g/L loading, (●) is 2g/L loading, and (▲) is 3g/L loading.

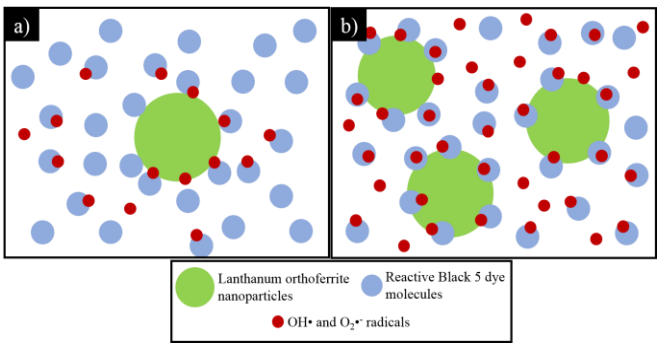

Fig. 5 Graphical comparison for the adsorption-photocatalytic reaction between different loadings: a) 1g/L and b) 3g/L of $LaFeO_3$

CONCLUSION

Comparative studies regarding the physicochemical properties and dye removal performance of lanthanum orthoferrite, $LaFeO_3$ synthesized by combustion method at two different reaction time have been reported. A rapid production of $LaFeO_3$(t=2h) nanoparticles exhibited bi-state amorphous-crystalline structure, based on XRD and TEM analyses, with high specific surface area. $LaFeO_3$(t=2h) nanoparticles showed an exceptional performance of RB5 dye removal, which successfully removed up to 94.39% of RB5 dye from the synthetic wastewater within 6h by synergistic adsorption-photocatalytic action. A lesser reaction time of $LaFeO_3$(t=2h) nanoparticles effectively reduced the operational cost and energy, making it a promising candidate in industrial and pharmaceutical wastewater treatment.

ACKNOWLEDGEMENT

This work was supported by the Malaysia Ministry of Education (MOE) under FRGS (Grant no: R.J130000.7851.5F007). The authors would also like to acknowledge Nagoya Institute of Technology and Japan Science and Technology Agency for financial support and instruments used for characterizations of samples within this study.

REFERENCES

[1] Ohtani, B. (2014). Revisiting the fundamental physical chemistry in heterogeneous photocatalysis: Its thermodynamics and kinetics. *Phys. Chem. Chem. Phys.*, 16:1788–1797. doi: 10.1039/C3CP53653J

[2] Castillo, N. C., Heel, A., Graule, T., Pulgarin, C. (2010). Flame-assisted synthesis of nanoscale, amorphous and crystalline, spherical $BiVO_4$ with visible-light photocatalytic activity. *Appl. Catal. B Environ*., 95:335–347. doi: 10.1016/j.apcatb.2010.01.012

[3] Thirumalairajan, S., Girija, K., Hebalkar, N. Y., Mangalaraj, D., Viswanathan, C., Ponpandian, N. (2013). Shape evolution of perovskite $LaFeO_3$ nanostructures: A systematic investigation of growth mechanism, properties and morphology dependent photocatalytic activities. *RSC Adv*., 3:7549–7561. doi: 10.1039/c3ra00006k

[4] Niu, T., Liu, G. L., Chen, Y., Yang, J., Wu, J., Cao, Y., Liu, Y. (2016). Hydrothermal synthesis of graphene-$LaFeO_3$ composite supported with Cu-Co nanocatalyst for higher alcohol synthesis from syngas. *Appl. Surf. Sci.*, 364:388–399. doi: 10.1016/j.apsusc.2015.12.164

[5] Mutalib, M. A., Aziz, F., Jamaludin, N. A., Yahya, N., Ismail, A. F., Mohamed, M. A.,…Yusof, N. (2018). Enhancement in photocatalytic degradation of methylene blue by $LaFeO_3$-GO integrated photocatalyst-adsorbents under visible light irradiation. *Korean Chem. Eng.,* 35:548–556. doi: 10.1007/s11814-017-0281-0

[6] Phokha, S., Pinitsoontorn, S., Rujirawat, S., Maensiri, S. (2015). Polymer pyrolysis synthesis and magnetic properties of $LaFeO_3$ nanoparticles. *Phys. B Phys. Condens. Matter.*, 476:55–60. doi: 10.1016/j.physb.2015.07.021

[7] Hao, X., Zhang, Y. (2017). Low temperature gel-combustion synthesis of porous nanostructure LaFeO3 with enhanced visible-light photocatalytic activity in reduction of Cr(VI). *Mater. Lett*. 197:120–122. doi: 10.1016/j.matlet.2017.03.133

[8] Parida, K. M., Reddy, K. H., Martha, S., Das, D. P., Biswal, N. (2010). Fabrication of nanocrystalline $LaFeO_3$: An efficient sol e gel auto-combustion assisted visible light responsive photocatalyst for water decomposition. *Int. J. Hydrog. Energy*, 35:12161–12168. doi: 10.1016/j.ijhydene.2010.08.029

[9] Qi, X., Zhou, J., Yue, Z., Gui, Z., Li, L. (2003). Auto-combustion synthesis of nanocrystalline $LaFeO_3$. *Mater. Chem. Phys.*, 78:25–29.

[10] Yin, H., Wada, Y., Kitamura, T., Kambe, S., Murasawa, S., Mori, H.,…Yanagida, S. (2001). Hydrothermal synthesis of nanosized anatase and rutile TiO_2 using amorphous phase TiO_2. *J. Mater. Chem.*, 11:1694–1703. doi: 10.1039/b008974p

[11] Shikha, P., Kang, T. S., Randhawa, B. S. (2015). Effect of different synthetic routes on the structural, morphological and magnetic properties of Ce doped $LaFeO_3$ nanoparticles. *J. Alloys Compd*. 625:336–345. doi: 10.1016/j.jallcom.2014.11.074

[12] Zhu, Y., Xu, S., Yi, D. (2010). Photocatalytic degradation of methyl orange using polythiophene/titanium dioxide composites. *React. Funct. Polym.* 70:282–287. doi: 10.1016/j.reactfunctpolym.2010.01.007

[13] Li, Y., Lu, A., Wang, C., Wu, X. (2008). Characterization of natural sphalerite as a novel visible light-driven photocatalyst. *Sol. Energy Mater. Sol. Cells.* 92:953–959. doi: 10.1016/j.solmat.2008.02.023

[14] Mazierski, P., Nischk, M., Gołkowska, M., Lisowski, W., Gazda, M., Winiarski, M. J.,…Zaleska-Medynska, A. (2016). Photocatalytic activity of nitrogen doped TiO_2 nanotubes prepared by anodic oxidation: The effect of applied voltage, anodization time and amount of nitrogen dopant. *Appl. Catal. B Environ.* 196:77–88. doi: 10.1016/j.apcatb.2016.05.006

[15] Shanavas, S., Priyadharsan, A., Vasanthakumar, V., Arunkumar, A., Anbarasan, P. M., Bharathkumar, S. (2017). Mechanistic investigation of visible light driven novel La_2CuO_4/CeO_2/rGO ternary hybrid nanocomposites for enhanced photocatalytic performance and antibacterial activity. *J. Photochem. Photobiol. A Chem.* 340:96–108. doi: 10.1016/j.jphotochem.2017.03.002

[16] Kanhere, P., Chen, Z. (2014). A review on visible light active perovskite-based photocatalysts. *Molecules*. 19:19995–20022. doi: 10.3390/molecules191219995

[17] Shet, A., Shetty, K. V. (2016). Photocatalytic degradation of phenol using Ag core-TiO_2 shell (Ag@TiO_2) nanoparticles under UV light irradiation. *Environ. Sci. Pollut. Res. Int.* 23:20055–20064. doi: 10.1007/s11356-015-5579-z

[18] Altman, I. S., Agranovski, I. E., Choi, M. (2005). Mechanism of nanoparticle agglomeration during the combustion synthesis. *Appl. Phys. Lett.* 87:5–8. doi: 10.1063/1.2005387